1.8 FLUX AGGREGATION OVER HETEROGENEOUS SURFACES IN A SEMI-ARID REGION : MODELLING AND VALIDATION

Y.H. Kerr (1)*, A. Chehbouni (2), L.H. Hipps (3), J. Schieldge (4), D.I. Cooper (5), W.E. Eichinger (6), R. Scott (7), D. C. Goodrich (8), J. Shuttleworth (7), K.H. Lee (7), C. Watts (9).

(1) CESBIO (CNES/CNRS/UPS), Toulouse, France;
(2) ORSTOM/IMADES, Hermosillo, Sonora, Mexico;
(3) Utah State Univ., Logan, UT;
(4) Jet Propulsion Lab., Pasadena, CA, USA;
(5) Los Alamos Nat. Lab., Los Alamos, NM, USA;
(6) Univ. of Iowa, Iowa City, IA USA;
(7) University of Arizona, Tucson, AZ, USA;
(8) USDA-ARS, Tucson, AZ, USA;
(9) IMADES, Hermosillo, Sonora, Mexico.

1. INTRODUCTION

The primary objective of the SALSA Program is to understand, model and predict the consequences of natural and human-induced change on the basin-wide water balance and ecological diversity of semiarid regions at event, seasonal, interannual, and decadal time scales (see Goodrich et al., 1998 ; this issue). The scientific objectives of the Salsa program are described in Goodrich et al., 1994. Among the scientific objectives there are the will to :

1. Improve the diagnosis of surface fluxes used in atmospheric models with grid spacings of several kilometers and compare remote and in-situ observations with real-time model runs, and ;
2. Develop and validate aggregation schemes with data taken over very highly heterogeneous surfaces.

To achieve these goals it is necessary to be able to model how to translate elementary fluxes (homogeneous patches) into aggregated fluxes compatible with model scales. This task requires to cope with two problems. The first one is to model the aggregation issue as the problem is not linear. The second is to validate the results. In this presentation we will show how we coped with these two issues and the very first results gained from the SALSA '97 campaign.

2. DATA SETS

2.1 THE STUDY AREA

The Upper San Pedro Basin (USPB) was identified as the focal area for initial SALSA research during the 1995 workshop noted above. In addition to those factors mentioned in the prior section, the basin embodies a number of characteristics which make it an exceptional outdoor laboratory to address a large number of scientific challenges in arid and semi-arid hydrology, meteorology, ecology, and social and policy science. The basin represents a transition area between the Sonoran and Chihuahuan deserts. It is an international basin spanning the Mexico-United States Border with significantly different cross border legal and land use practices, significant topographic and vegetation variation, and a highly variable climate.

The annual rainfall ranges from around 300 mm to 750 mm with the majority of annual precipitation (~65%) occurring during the July through September monsoon season from high intensity air-mass convective thunderstorms and roughly 30% coming from less intense winter frontal systems. Potential evapotranspiration is high, estimated at over ten times annual rainfall. Major vegetation types include desert shrub-steppe, grasslands, oak savannah, pinyon-juniper, and ponderosa pine. In portions of the basin all of these vegetation types are contained within a 20 km span.

As we had to start working on the aggregation issue before all of the measurements were performed and available, we started to work with the HAPEX SAHEL data set. Hapex Sahel took place in 1992 in Niger (see HAPEX SAHEL Journal of Hydrology special issue, 1997). The area has a very similar climate to that of the USPB. The vegetation is very patchy but with a limited variety of land use. The area is essentially flat and the rainfall pattern is concentrated during the « monsoon » period which extends from mid June to end of September.

2.2 MEASUREMENTS

HAPEX SAHEL :

The measurements performed during Hapex Sahel are described in Prince et al., 1995. They consisted mainly in characterisation of the surface components (soils, vegetation type and density), measurements energy and water fluxes (rainfall, storage [ground water and ponds], sensible and latent heat fluxes, net radiation and ground flux, air and surface temperature, soil moisture profiles, etc...). The ground measurements were performed mainly over three so called « supersites ».

Meteorological measurements and radiosoundings were done at several locations over the square degree area. Aircraft measurements were also performed during the intensive observation period (remote sensing and fluxes). Finally satellite acquisitions were collected on an almost routine fashion. An overview of the data collected can be found on the WEB site « http ://www .orstom.fr/hapex ».

SALSA '97 :

Experimental surface observations were obtained from a variety of existing as well as newly initiated data collection activities that were integrated into the 1997 SALSA Program activities. We worked mainly with the Lewis Spring site in the USA data as well as with the Zapata site in Mexico (see Goodrich et al., 1998 this issue). The sites have sparse desert grass cover and a wide variety of in-situ and remotely sensed data. These measurements include basic meteorology, energy and CO2 fluxes, soil moisture, vegetation sampling, and surface reflectances/emittance. We worked mainly with the data collected during the August 1997 campaign, when additional instrumentation deployed included an array of eddy correlation flux instrumentation (see ET summary by Hipps et al., this issue), the scintillometer, and the Las Alamos National Laboratory Raman LIDAR system (Cooper et al., this issue). The main innovation in the measurements consisted in an attempt to use scintillometry to quantify fluxes over scales compatible with models (McAnnaney et al., 1995 ; Green et al., 1997) .

3. METHODS

3.1 MODELLING

The modelling approach used for aggregation is that described in Chehbouni et al., and can be described as follows. The basis is the classical equation R_N=H + LE + G where R_N is the net radiation, H the sensible heat flux LE the latent heat flux and G the ground flux. This equation can be written, after expressing the different terms :

$$\rho C_p \frac{T_s - T_a}{r_a} + \frac{\rho C_p}{\gamma} \frac{e_{sat}(T_s) - e_a}{r_a + r_s} + G - (1-\alpha)R_g - \varepsilon\left(L\downarrow - \sigma T_s^4\right) = 0 \quad (1)$$

Where ρ is the density of air, C_p the heat capacity at constant pressure, T_s the surface temperature, T_a the air temperature, r_a the aerodynamic resistance, γ the psychrometric constant, r_s the stomatal resistance, R_g the shortwave downward flux, ε the emissivity, $L\downarrow$ the downward longwave flux, σ the Stefan Boltzmann constant. Equation (1) Is considered as valid both at « large scale » and locally.We will thus see how to translate the « local » coefficients to large scale ones.

It is first assumed that the vegetation cover is known. This is achieved using either ground characterisation or remotely sensed data which allows to quantify vegetation fraction cover. In a first step, it is also assumed that the atmospheric characteristics remain constant (wind speed, air temperature). . The water vapour deficit $\Delta e_{sat} = e_{sat}(T_a) - e_a$ is usually introduced in the difference

$$e_{sat}(T_s) - e_a$$

after linearisation :

$$e_{sat}(T_s) - e_a = e_{sat}(T_s) - e_{sat}(T_a) + e_{sat}(T_a) - e_a$$

giving

$$e_{sat}(T_s) - e_a = s(T_s - T_a) + \Delta e_{sat} \quad (2)$$

where s represents the slope of the curve of saturation vapour pressure at temperature T_a. Hence,

$$LE = \frac{\rho C_p}{\gamma} \frac{s(T_s - T_a) + \Delta e_{sat}}{r_a + r_s} \quad (3)$$

Surface temperature is also linearised:

$$T_s^4 = T_a^4 + 4T_a^3(T_s - T_a) \quad (4)$$

After some calculations the energy budget can be written :

$$\rho C_p \left[\frac{T_s - T_a}{w} + \frac{\Delta e_{sat}}{\gamma(r_a + r_s)}\right] - (1-\alpha)R_g - \varepsilon R_L + G = 0 \quad (5)$$

with w et R_L given by :

$$\frac{1}{w} = \frac{1}{r_0} + \frac{1}{r_a} + \frac{1}{\gamma(r_a + r_s)} \quad (6)$$

$$R_L = L\downarrow - \sigma T_s^4 \quad (7)$$

and r_0 ,the resistance to radiative transfer :

$$r_0 = \frac{\rho C_p}{4\varepsilon\sigma T_a^3} \qquad (8)$$

For a given type of vegetation i we have :

$$\rho C_p\left[\frac{T_{si}-T_a}{w_i}+\frac{\Delta e_{sat}}{\gamma\left(r_{ai}+r_{si}\right)}\right]- \qquad (9)$$
$$\left(1-\alpha_i\right)R_g-\varepsilon_i R_L+G_i=0$$

After summation over all the vegetation types we have :

$$\rho C_p\left[\sum_i a_i\frac{T_{si}-T_a}{w_i}+\sum_i a_i\frac{\Delta e_{sat}}{\gamma\left(r_{ai}+r_{si}\right)}\right]$$
$$-\sum_i a_i\left(1-\alpha_i\right)R_g-\sum_i a_i\varepsilon_i R_L \qquad (10)$$
$$+\sum_i a_i G_i=0$$

Since the energy budget is validated over the whole area we do an identification term by term which gives :

$$T_s = w\sum_i\frac{a_i T_{si}}{w_i} \qquad (11)$$

$$\frac{1}{w}=\sum_i\frac{a_i}{w_i} \qquad (12)$$

$$\frac{1}{r_a+r_s}=\sum_i\frac{a_i}{r_{ai}+r_{si}} \qquad (13)$$

$$G=\sum_i a_i G_i \qquad (14)$$

$$\alpha=\sum_i a_i\alpha_i \qquad (15)$$

$$\varepsilon=\sum_i a_i\varepsilon_i \qquad (16)$$

by combining equations (6), (8), (12) et (16) we get :

$$\frac{1}{r_a}=\sum_i\frac{a_i}{r_{ai}} \qquad (17)$$

$$\frac{1}{r_0}=\frac{4\sigma T_a^3}{\rho C_p}\sum_i a_i\varepsilon_i \qquad (18)$$

This approach allows to compute the resistances and surface temperatures over an area covered with heterogeneous vegetation. From the equations, it is easy to derive the latent and heat fluxes (equations 2 and the classical $H=\rho C_p\frac{T_s-T_a}{r_a}$).

It must be noted that, as expected, the fluxes are not straightforward surface weighted averages. On point of concern is the validity of the linearisation $e_{sat}(T_s)-e_a$ which is not valid when T_s and T_a are significantly different. And this phenomenon occurs frequently around midday. In such cases, as the vapour saturation pressure is an exponential function the linearisation induces errors equal to :

$$\Delta=\left[e_{sat}(T_s)-e_{sat}(T_a)\right]-\left[s(T_s-T_a)\right]$$

for a 10 K difference between T_s and T_a the error induced reaches 20%. As this error translates directly into the latent heat flux, it has a significant impact on the model output. Consequently we did not use the linearised formula in the computations.

3.2 SCINTILLOMETER

The approach taken is that of McAnneney et al., 1995. The instrument used was made by the department of Meteorology of the University of Wageningen. The method relies on the measurement of structure parameter C_n^2 over the path length (about 600 m in our case), which corresponds to an integrated value weighted by a bell shaped function. The structure parameter for temperature can be written:

$$C_T^2 = C_N^2\left(\frac{T_a^2}{\gamma P}\right)^2\left(1+0.03/\beta\right)^2 \qquad (18)$$

Where β is the bowen ratio, P the atmospheric pressure, T_a the air temperature and $\gamma = 7.9\ 10^{-7}\ KPa^{-1}$. C_T^2 et T* are linked trough the relationship where z is the height of measurement minus the displacement height :

$$C_T^2 = T_*^2 z^{-2/3} f\left(\frac{z}{L}\right) \qquad (19)$$

The expressions for f vary according to different authors, we used those of Wyngaard (1973) :

for unstable conditions ($z/L \leq 0$)

$$f(\frac{z}{L}) = 4.9\left(1 + 7\left|\frac{z}{L}\right|\right)^{-2/3} \quad (20)$$

for stable conditions ($z/L \geq 0$)

$$f(\frac{z}{L}) = 4.9\left(1 + 2.4\left|\frac{z}{L}\right|^{2/3}\right) \quad (21)$$

L is Monin-Obhukov length given by :

$$L = -\frac{T_a u_*^2}{k g T_*} \quad (22)$$

with k = 0.4 (Karmann constant) et g = 9.81 ms^{-2} (gravity)
Knowing the displacement and roughness lengths and a first guess of L we can compute u*:

$$u^* = \frac{kU}{\ln\left(\left(\frac{z}{z0}\right) - \varphi(\frac{z}{L})\right)} \quad (23)$$

with U the wind speed and

$$\varphi = \ln\left[(1+\chi 2)(1+\chi)^2 \frac{1}{8}\right] - 2\,Arc\tan(\chi) + \frac{\pi}{2} \quad (24)$$

$$\chi = \left(\frac{1-16z}{L}\right)^{1/4} \quad (25)$$

Knowing u* and C_T^2 (equation 18) as well as T* (eq 19). Then H follows from

$$H = \rho\, c_p\, u_* T_* \quad (26)$$

This gives a derived value for z/L knowing that

$$\frac{z}{L} = \frac{-zgkT^*(1+0.07\beta)}{u^{*2}\,T} \quad (27)$$

The procedure is then repeated until z/L converges. If the net radiation and soil heat flux are known, on can also iterates on the retrieved value of H to assess the Bowen ratio (many authors neglect it) but the process becomes computationally demanding.

Or free convection conditions one can also use following Kohsiek (1982) and De Bruin et al. (1995) the following expression :

$$H = \rho\, c_p\, b\, z\left(\frac{g}{T_a}\right)^{1/2} \left(C_T^2\right)^{3/4} \quad (28)$$

where b = 0.57.

4. PRELIMINARY RESULTS

Work presented in this paper corresponds only to very preliminary results. Actually, we simply tested the approach on the HAPEX SAHEL data set and intend to validate it more extensively on the SALSA data where we will have access to scintillometer measurements. It must also be stated that a full validation will require the analysis of data collected over an area with contrasted conditions.

To test the results we compared the surface temperature computed with the above mentioned approach to the surface averaged temperature. The results are given below in table 1. The fourth column gives the average temperature difference between the two methods, the fifth the standard deviation and the last one the maximum value encountered, all are expressed in percentage with regard to the surface averaged temperature.

Table 1 Surface temperature

DATE	mean (%)	STD (%)	max (%)
1/09/92	0,51	0,62	2,21
3/09	2,66	1,14	4,76
4/09	1,14	0,93	3,94
5/09	3,69	2,27	6,37
6/09	4,91	3,37	9,58
7/09	4,45	4,59	13,24
10/09	1,58	1,68	4,93
14/09	3,40	2,97	9,34
16/09	2,53	2,07	6,78
Mean	**2,77**	**2,18**	**6,80**
STD	**1,50**	**1,28**	**3,40**

One can see that the temperature difference is not significantly high (2 to 3 %) which correspond to the rather uniform surface conditions. However, it can reach high values (13% which amounts to 5 K).

The same comparison method was applied to the sensible heat flux, and is depicted on figure 2. Again the average is not very high (5%) but we found a high standard deviation (7%), and correspondingly, high values for the extreme differences, which can reach 30% of the flux.

Table 2 sensible heat flux

Date	Mean(%)	STD (%)	max (%)
1/09/92	3,72	4,92	12,66
3/09	4,22	5,94	16,73
4/09	4,48	6,20	17,45
5/09	4,30	5,68	20,91
6/09	3,38	4,28	10,97
7/09	6,57	8,09	20,93
10/09	5,06	5,74	17,63
14/09	9,25	10,66	25,13
16/09	8,06	11,23	31,09
Mean	**5,45**	**6,97**	**19,28**
STD	**2,05**	**2,48**	**6,17**

Table 3 Latent heat flux

Date	Mean (%)	STD (%)	MAX (%)
1/09/92	2,04	2,58	7,21
3/09	4,46	5,29	11,42
4/09	3,54	2,96	8,06
5/09	9,91	2,75	14,60
6/09	9,31	2,78	13,04
7/09	6,99	3,45	15,47
10/09	8,40	7,36	19,14
14/09	3,82	4,79	10,05
16/09	2,82	3,56	7,10
Mean	**5,70**	**3,94**	**11,79**
STD	**2,98**	**1,59**	**4,14**

Finally, we compared the composited and surface averaged latent heat fluxes (table 3). If the mean value of the difference is very close to that of the sensible heat flux, the standard deviation is much lower as for the maximum difference.

This study shows that the simple surface averaged temperature and fluxes may be significantly different. The next question is thus to identify which one is closest to reality. For this we investigated the use of the AVHRR for temperature and MERLIN data for fluxes. With the AVHRR we did not have much success since the dates when we had all the ground measurements were often cloudy at the time of overpass. Secondly we had only access to averaged surface temperatures and it was difficult to relate them to the instantaneous AVHRR measurement. The aircraft acquisitions gave us also mixed feelings. It seems that there is a constant overestimation (whichever the method, including measured fluxes) of ground fluxes vs aircraft fluxes. Consequently the uncertainties do not allow to draw any conclusions as the A/C fluxes are way out of the results from either the model or the surface averaged fluxes. We intend to use the sensible heat flux measured with the scintillometer to verify our model.

Table 4 comparison of results for varying cover (percentage of change)

Temperature

fallow/millet	1/12	1/6	1/4	1/3	5/12
1/12	4,5	3,7	2,9	2,3	1,8
1/6	2,7	1,9	1,3	0,9	0,9
1/4	1,2	0,6	0,0	0,6	1,1
1/3	0,9	0,8	1,1	1,6	2,0
5/12	1,4	1,7	2,1	2,5	2,9

Sensible Heat Flux

fallow\millet	1/12	1/6	1/4	1/3	5/12
1/12	16,8	11,5	7,8	7,9	11,2
1/6	13,0	7,7	3,7	5,5	9,8
1/4	10,5	5,1	0,0	4,9	9,5
1/3	9,9	5,3	3,5	6,9	11,0
5/12	10,4	7,1	6,7	9,4	13,1

Latent heat flux

fallow/millet	1/12	1/6	1/4	1/3	5/12
1/12	26,8	20,0	13,6	7,7	4,1
1/6	19,0	12,7	6,6	2,0	5,8
1/4	11,9	5,8	0,0	5,6	11,1
1/3	5,8	2,0	6,4	11,7	16,9
5/12	4,1	7,5	12,5	17,7	22,7

Finally we checked the sensitivity of the two approaches to the accuracy of the surface cover estimates. For this we changed the percentage of cover for millet and fallow and compared the results as shown in table 4. Taking as a reference an area with 25% millet, 25 % fallow and 50 % bare soil, we changed the proportions to 8, 17,25, 33,42 % for each vegetation component. The bare soil proportion varying accordingly. The number corresponds to the change of the considered parameter in percent. The results shown are the means for 9 days (same days as in table 1 to 3). As expected in such environment, the most important effect is that of bare soil for temperature. However the mean variation is less than 2 °C on average, but it can reach 4°C for maximum difference and extreme error in surface cover. For sensible and latent heat fluxes, the role of surface cover is somewhat larger as it can reach 27% change. Moreover it can be

seen on the tables that for the same amount of bare soil, the respective contributions of fallow and millet are no more negligible.

In conclusion, one may say, that even if an extreme accuracy is not required, a good knowledge of surface cover is nevertheless required.

5 CONCLUSION

This paper presents the very first results from our attempt to model aggregation. We found that there were differences between our model and an area weighted average. We also found that with our model, as expected, surface cover had to be known. Unfortunately, it is not yet possible from the data we had to decide which was the most accurate method. We believe that with the data collected last august on the ground and with the scintillometer, will enable us in the near future to select the most appropriate method and validate it.

6. ACKNOWLEDGMENTS

Financial support from the USDA-ARS Global Change Research Program, USDA National Research Initiative Grant Program, Electrical Power Research Institute, Arizona Department of Water Resources, U.S. Environmental Protection Agency - Office of Research and Development, CONACYT, ORSTOM, the French Remote Sensing Program (PNTS) via the VEGETATION Project and the ERS2/ATSR2 Project, and US Bureau of Land Management is gratefully acknowledged. Assistance was also provided in part by the NASA/EOS grant NAGW2425, EPA STAR Graduate Student Fellowship Program, National Science Foundation, US Geological Survey, US Department of Energy contract W-7405-ENG-36, California Institute of Technology-Jet Propulsion Laboratory (NASA, EOS/ASTER), WAU (Wag. Agricultural University, Netherlands); this support is also gratefully acknowledged. Special thanks are extended to the ARS staff located in Tombstone, Arizona for their diligent efforts. This work was performed in the framework of the French team effort for EOS/MTPE. We are very thankful to J.P. Lagouarde and J. McAneney for sharing with us their large expertise on scintillometry.

7. REFERENCES

Chehbouni A. et al., 1995. Approaches for averaging surface parameters and fluxes over heterogeneous terrain. *Journal of climate*. Vol 0. P 1-8.

De Bruin H.A.R., Van Den Hurk B.J.J.M., Kohsiek W., 1995 : The scintillation method tested over a dry wineyard area. *Boundary-Layer Meteorol.*, 76, 25-40.

Goodrich, D. C., 1994: SALSA-MEX: A Large Scale Semi-Arid-Land-Surface-Atmospheric Mountain Experiment. Proc. 1994 Intern. Geoscience and Remote Sensing Sym. (IGARSS'94), Pasadena, CA, Vol. 1, Aug. 8-12, p. 190-193.

Green A.E., McAneney K.J., Lagouarde J.P., 1997 : Sensible heat and momentum flux measurement with an optical inner scale meter. *Agric. For. Meteorol.*, 85, 259-267.

Hill R.J., Ochs G.R., Wilson J.J., 1992 : Surface-layer fluxes measured using the C_T^2-profile method. *J. of Atmospheric and Oceanic Technology*, 9, 5, 526-537.

Journal of hydrology, Special issue on Hapex Sahel, guest Eds Goutorbe, Dolman, Gash, Kerr, Lebel, Prince, Stricker, **188-189**, no. 1-4.

Kohsiek W., 1982 : Measuring C_T^2, C_Q^2 and C_{TQ} in the unstable surface layer, and relations to the vertical fluxes of heat and moisture. *Boundary-Layer Meteorol.*, 24, 89-107.

McAneney K.J.,et al., 1995 : Large-aperture scintillometry : the homogeneous case. *Agric. For. Meteorol.*, 76, 149-162.

Prince, S.D.et al., 1995, Geographical, Biological and Remote Sensing Aspects of the HAPEX SAHEL: *Remote Sens. Envir.*, v. 51, p. 215-234.

Wyngaard J.C., 1973 : On surface-layer turbulence.Workshop on Micrometeorology, Denver, Colorado, Amer . Meteor. Soc., 101-149.

REFERENCES IN THIS ISSUE

Chehbouni, A., O. Hartogensis, L. Hipps, J-P. Brunel, C. Watts, J. Rodriguez, G. Boulet, G. Dedieu, Y. Kerr, and H. De Bruin, (a) Sensible heat flux measurements using a large aperture scintillometer over heterogeneous surfaces.

Cooper, D.I., W. Eichinger and L. Hipps, Spatial properties of water vapor scalar and flux over a riparian corridor.

Goodrich, D.C. et al, An overview of the 1997 activities of the Semi Arid Land Surface Atmosphere (SALSA) program.

Hipps, L.E., D. Cooper, W. Eichinger, D. Williams, S. Schaeffer, K. Snyder, R. Scott, A. Chehbouni, C. Watts, O. Hartogensis, J-P. Lhomme, B. Monteny, J-P. Brunel, G. Boulet, J. Schieldge, H. De Bruin, J. Shuttleworth, and Y. Kerr, A summary of processes which are connected to evaporation of riparian and heterogeneous upland vegetation in arid regions.

PREPR

78TH AMS ANNUAL MEETING
11-16 JANUARY 1998

SPECIAL SYMPOSIUM ON HYDROLOGY

11–16 JANUARY 1998

PHOENIX, ARIZONA

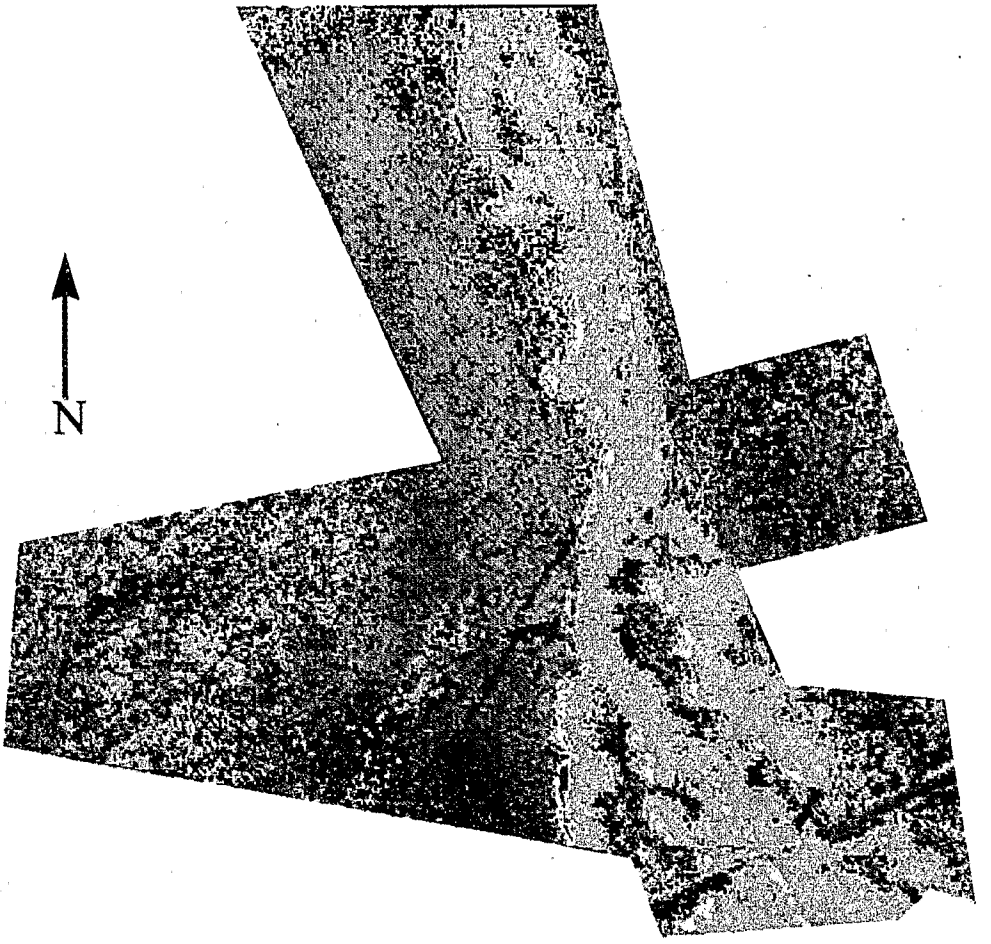

scale 1:6950

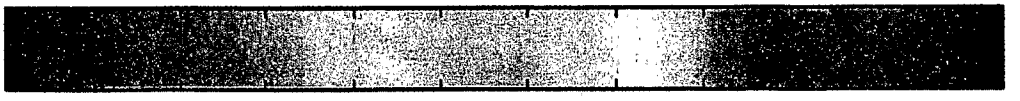

RIPARIAN ET FROM THE SALSA PROGRAM

AMERICAN METEOROLOGICAL SOCIETY